



Influence of structure on the aseismic stability and dynamic responses of liquefiable soil

Pengfei Dou¹ · Chengshun Xu¹ · Xiuli Du¹ · Su Chen²

Received: 9 March 2021 / Accepted: 24 August 2021 / Published online: 22 September 2021
© The Author(s), under exclusive licence to Springer Nature B.V. 2021

Abstract

In previous major earthquakes, the damage and collapse of structures located in liquefied field which caused by site failure a common occurrence, and the problem of assessment of liquefaction possibility and discussion on the seismic response and stability of liquefied site is still issue of common concern in geotechnical earthquake engineering. To study the influence of the existence of structure on the seismic responses and stability of liquefiable sites, two groups of shaking table tests on liquefiable non-free field (with structure) and a free field (without structure) are performed. It can be summarized from the experimental results as following. The natural frequency of non-free field is larger and the damping ratio is smaller than that of a free field. For the weak seismic loading condition, the dynamic response of sites shows similar rules and trend. For the strong ground motion condition, soils in both experiments all liquefied obviously and the depth of liquefaction soil in the free field is significantly greater than that in the non-free field, besides, porewater pressure in the non-free field accumulated relately slow and the dissipated quickly from analysis of porewater pressure ratios in both experiments. The amplitudes of lateral displacements and acceleration of soil in the non-free field are obviously smaller than that in the free field caused by the effect of presence of the structure. In a word, the presence of structures will lead to the increase of site stiffness, site more difficult to liquefy, and the seismic stability of the non-free site is higher than that of the free site due to soil–structure interaction.

Keywords Free field · Non-free field · Shaking table tests · Dynamic response · Porewater pressure · Seismic stability

1 Introduction

As early as 1964, during the Alaska earthquake in USA and the Niigata Earthquake in Japan, the foundation bearing capacity reduction, uneven settlement and lateral spreading caused by soil liquefaction lead to the overturning and collapse of structures observed in

✉ Chengshun Xu
xuchengshun@bjut.edu.cn

¹ Key Laboratory of Urban Security and Disaster Engineering of Ministry of Education, Beijing University of Technology, Beijing 100124, China

² Institute of Geophysics, China Earthquake Administration, Haidian District, Beijing 100081, China

the post-earthquake investigation. In previous major earthquakes, foundation failure due to liquefaction of sand and soil was observed, resulting in the destruction of buildings caused by then. In the 1994 Ms6.8 Northridge earthquake in California (Youd and Garris 1995; Holzer et al. 1999), extensive, slowly dipping alluvial fan surface permanent deformation, cracks were appeared in the San Fernando Canyon. In 1999, the Mw7.4 Kocaeli earthquake in Turkey caused a large area of Izmit Bay area to liquefy and caused lateral slip (Sonmez and Ulusay 2008). Besides, 20% of the 3–6-story concrete houses and 56% of the 1–2-story brick and wood houses in Adapazari City were seriously damaged or destroyed due to the liquefaction of the foundation in this major earthquake (Cetin et al. 2004). In the 2012 Italian earthquake, by analyzing the correlation between structural damage and site liquefaction, it is found that liquefaction has a significant effect on the destruction and collapse of buildings (Ludovico et al. 2020).

Liquefied soil–structure dynamic system damaged under seismic loadings is not only related to the dynamic characteristics of soil or the structure, but also related to the change of mechanical properties of sand soil after liquefaction, the deformation behaviors at the contact surface of soil and structure as well as the transfer mechanism of interaction forces. In particular, the soil natural frequency decreases after triggering liquefaction (Kramer et al. 2016; Lombardi and Bhattacharya 2014, 2016). In fact, the problems of soil–structure dynamic interaction under seismic loadings should be more complicated involving the liquefaction of saturated sand (National Research Council 1985), and many scholars have carried out a large number of studies on the liquefaction possibility discrimination of saturated sandy soil, liquefied soil–structure dynamic interaction and foundation failure of liquefied site by means of numerical calculation model (Li and Motamed 2017; Qiu et al. 2019; Horikoshi and Thakareet 2003; Mokhtar et al. 2014), various experimental techniques (Haeri et al. 2012; Motamed et al. 2009; Tabata and Sato 2010; Suzuki et al. 2005; Su et al. 2015; Gao et al. 2011) and theoretical method an analysis (Naggar and Novak 1994a, b; Elsayy et al. 2019; Boulanger et al. 1991; Varun 2012), and the seismic responses of various structures in liquefaction site were discussed in detail. Therefore, study on soil liquefaction and soil–pile–structure dynamic interaction in saturated soil sites under seismic loadings is still an important research topic in geotechnical earthquake engineering, and the evaluation of liquefaction possibility and risk as well as the discussion of foundation failure due to soil liquefaction are the main aspects of scientific problems related to liquefaction.

In the aspect of liquefaction identification, the estimation of liquefaction of saturated sand site has always been one of the main problems in the study of soil dynamic characteristics. At present, the assessment methods of site liquefaction mainly include the critical standard penetration number method (Seed et al. 1985), the cyclic stress method (Dobry et al. 1982), the wave velocity method (Seed and Idriss 1971), the energy method (Davis and Berrill 1982a), and the uncertainty evaluation method based on the probabilistic neural network of fuzzy mathematics (Chen and Li 2006). Among them, assessment methods of liquefaction proposed by Seed (Seed et al. 1983; Youd et al. 2001; Fukutake et al. 1990; BS En 1998-5 2004) has been most widely used after continuous improvement and refinement. These assessment methods are based on the characteristics of soil and ground motion parameters under free field conditions to carry out the possibility of liquefaction and liquefaction hazard analysis. However, in the actual engineering sites, because buildings or structures are in a certain site, soil–structure dynamic interaction will significantly change the stress, drainage conditions and seismic responses of the soil near the structure and also affect the characteristics of seismic wave propagation in soils, and then affect the structure around the soil liquefaction possibility and the dynamic response characteristics of the liquefaction (Du and Lu 2011; Chiaradonna et al. 2020). Therefore, it is difficult to proceed

with accurate assessment of liquefaction possibility and to predict seismic responses of saturated sand in the non-free site. The accurate assessment of the liquefaction possibility of saturated sand is related to the following analysis and correct understanding on the site stability of the building foundation under seismic loadings.

Global numerical models of liquefiable site–structure system are established by using finite element method, finite difference method and other numerical analysis methods, especially the method of elastic–plastic effective stress analysis with drainage and undrained, and numerical analysis models can consider soil–structure interaction, and the development of porewater pressure, stress and strain as well as dynamic responses of soil liquefaction process. It is an efficient method to analyze and evaluate the liquefaction possibility of saturated sandy soil via the simulation results of the numerical analysis model. Yiagos (Yiagos and Prevost 1991) established the dynamic elastoplastic analysis method of earth–rock dam by using the elastic–plastic constitutive relationship of effective stress multiple yield surface functions following dynamic hardening. The nonlinear hysteretic characteristics of the soil skeleton and the relationship between dilatancy and effective stress ratio were simulated, and the effects of pore water pressure and other problems on liquefaction-related were also discussed. Dafalias and Manzari (2004) built a stress-ratio controlled, critical state compatible sand model, which takes into account the effect of fabric changes in the multi-axial generalization, and this constitutive model has been implemented in the finite-difference software FLAC3D (Cheng et al. 2013) and applied in the analysis of liquefaction problems (Ramirez et al. 2018), achieving good simulation results. In addition, Morz et al. (1981) and Pastor et al. (1990) have also carried out in-depth research on elastic–plastic analysis methods. Elastic–plastic analysis method is more in line with the real property of soil in theory, so it has been paid more attention by more scholars and developed more rapidly in recent years. However, on the whole, the global numerical analysis and simulation methods still have some shortcomings, such as large computational workload, complicated numerical algorithm and difficult to determine the parameters.

As a reliable research method of geotechnical engineering, shaking table test technology has been widely used in studying on the problems of soil–structure dynamic interaction, seismic response of liquefaction site, etc. (Haeri et al. 2012; Motamed et al. 2009, 2010; Motamed and Towhata 2010a, b; Tabata and Sato 2010; Suzuki et al. 2005; Su et al. 2015; Gao et al. 2011; Tobita et al. 2004; Li 2011; Matsumoto et al. 2004; Stringer and Madabhushi 2011, 2013; Haldar and Babu 2010; Chen et al. 2015; Hayashi and Kaneda 2019; Okamura and Teraoka 2006; Ye et al. 2006; Varghese and Latha 2014; Shamy et al. 2010; Tsai et al. 2016; Hadush et al. 2000; Sasaki et al. 1992; Xu et al. 2020a, b). Li (2011) carried out centrifuge tests of a 2×2 pile group configuration of stainless steel tubular piles on the dynamic performance of pile group foundation under horizontal load, and the different dynamic performances of bored and jacked piles under cyclic load are studied to discuss the influence of different pile installation methods on lateral dynamic responses of piles. Stringer et al. (Matsumoto et al. 2004) conducted similar centrifuge shaking table tests to explore the effect of pile formation on pile group settlement. Matsumoto et al. (Stringer and Madabhushi 2011) conducted a series of 1-g shaking table tests on a pile raft foundation in Toyoura dry sand, and the main frequency of input seismic record and dynamic characteristics of the superstructure as two experimental variables are considered. The results show that inclination of the raft foundation, shear forces and bending moments of piles are all related to the two experimental variables.

In previous studies, most dynamic catastrophe process studies involving liquefied soil–structure dynamic system under seismic loadings just focused on the earthquake response of pile foundation or superstructures as a research expatiates (Li

2011; Matsumoto et al. 2004; Stringer and Madabhushi 2011; Haldar and Babu 2010; Chen et al. 2015; Motamed and Towhata 2010a, b; Motamed et al. 2010; Hayashi and Kaneda 2019), or analyzed and discussed soil liquefaction mechanism and site failure as well as liquefaction spreading problems only from the perspectives on the soil liquefaction features or seismic responses of the free site (Okamura and Teraoka 2006; Ye et al. 2006; Varghese and Latha 2014; Shamy et al. 2010; Tsai et al. 2016; Hadush et al. 2000; Sasaki et al. 1992). For example, Okamura and Teraoka (2006) conducted a shaking table test of liquefiable free field to study the possibility of desaturation method as an anti-liquefaction measure adopting to prevent soil liquefaction. Ye et al. (2006) has carried out one group of shaking table test to discuss the dynamic characteristics of soil after liquefaction. By using sensors buried in soil, the difference of the characteristics of soil before and after liquefaction can be reflected though recording the propagation velocity of wave in the soil before and after the model of hitting the bottom. The experimental results show that the liquefaction will occur again even under the same ground motion input, and the seismic response will also be different when soils liquefy again. Varghese and Latha (2014) conducted a series of shaking table tests to study the liquefaction characteristics of free field site. The test results show that the liquefaction of soil depends on the characteristics of ground motion to a large extent: the higher the peak acceleration, the easier the liquefaction of soil; besides, the increase in the dead weight earth pressure of overburden soil layer also makes it more difficult for soils tending to liquefy.

However, there are few studies on the influence of the existence of structures on liquefaction behaviors and seismic stability of site soil. Seismic stability of liquefiable sites refers to the property of site soil to resist ground damage caused by earthquakes, such as ground cracks, landslides, lateral spreading and collapses, etc., which is mainly reflected in the acceleration and displacement response as well as the pore pressure response of liquefied soil under earthquake loadings. Besides, in these previous research, there are conflicting studies on whether the presence of the structure makes the surrounding saturated sand more susceptible to liquefaction and how it affects the dynamic response of the site after liquefaction. Some scholars (Li and Motamed 2017; Stringer and Madabhushi 2013) believe that the existence of the structure will make the site more prone to liquefaction, because it is observed that the pore pressure of soil near the structure rises quickly but dissipates slowly, but other studies (Huang et al. 2005; Zhuang et al. 2015) suggest the opposite.

In this paper, two groups of large shaking table tests are carried out for discussing on the influence of the structure on the seismic stability of liquefiable sites. By comparing the experimental results from the free field and non-free field experiments, such as the dynamic characteristics, acceleration response, the rules of porewater pressure ratios in saturated sand layer, soil lateral displacements, etc., the influence of the existence of the structure on the dynamic characteristics and seismic stability of the liquefiable site is analyzed and summarized. The purpose of this paper is to qualitatively analyze the seismic response of the site soil in the existence of the structure by carrying out a series of shaking table tests, especially the pore pressure and acceleration response. Besides, the other purpose is to discuss the comprehensive effect of the existence of structures on the liquefaction behavior, and to improve the understanding on the difference between the soil properties or the ground motion propagation characteristics in the free field and in the presence of the structure, in the analysis of liquefaction possibility and risk.

2 Description of shaking table test

Contents of experimental design scheme, include the chosen shaking table, similar ratio design, the laminar shear soil container, etc., have been introduced in Reference Xu et al. (2020a, b) in detail. In order to facilitate understanding of the test results analysis in this paper, in the following introduction of the test scheme, only the model system setting, sensor layout, loading conditions and other contents are introduced as necessary.

Figure 1 presents a schematic drawing of the whole test package for the pile group-superstructure in either the free field or the non-free field on the shaking table. In this series of shaking table experiments, the model sites are all consisted of the same stratified soils, with 0.5 m dense sandy soil layer, 1.2 m loose sand layer (i.e. saturated sandy soil layer) and 0.3 m clay crust layer, successively from bottom to top. The pile group consisted of four piles placed in a 2×2 configuration, and the superstructure is a simplified structure composed of two lumped masses. The natural vibration frequency of the structure is approximately 0.7 s.

Live-action on shaking-table in Experiment-NF is shown in Fig. 2. Figure 3 is layout of test package and instrumentation in both experiments.

The model pile group consisted of four piles placed in a 2×2 configuration; each was 1700 mm long and 100 mm in diameter. The piles were embedded 400 mm into the dense sand layer (i.e. four times the pile diameter). The center-to-center spacing between piles was five times the pile diameter. The piles were connected to the pile cap through four corresponding holes with diameter 102 mm, which was $0.8 \text{ m} \times 0.8 \text{ m} \times 0.25 \text{ m}$. Thus, piles were embedded 1650 mm in the model soil and inserted 50 mm into the pile cap through the four reserved holes. The pile cap was embedded in the clay, and the upper surface of it was flush with the soil surface. The superstructure comprised two relatively rigid blocks connected by a flexible column. The mass of each rigid block was 410 kg and the total mass of the simplified superstructure was 900 kg approximately. The two steel blocks were connected to the pile cap with a 3 m long steel column made of H-section as illustrated in Figs. 2 and 3.

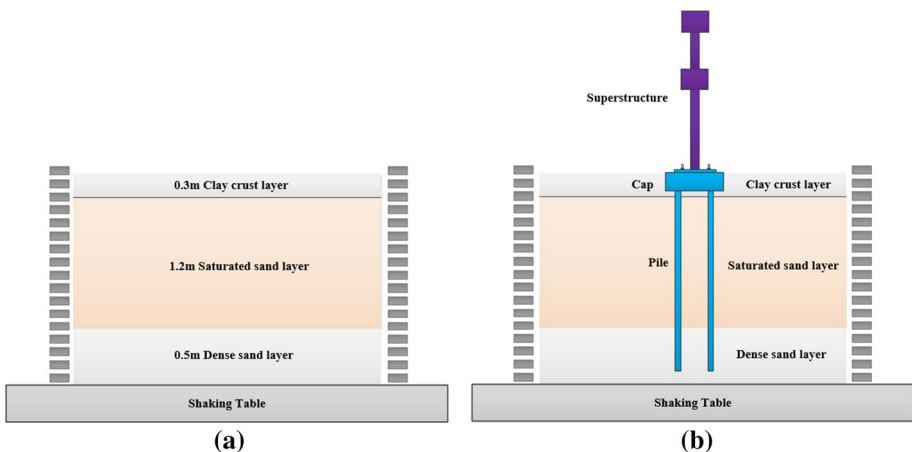


Fig. 1 Model systems in two experiments: **a** Experiment-F; **b** Experiment-NF

Fig. 2 Live-action on shaking-table in the Experiment-NF

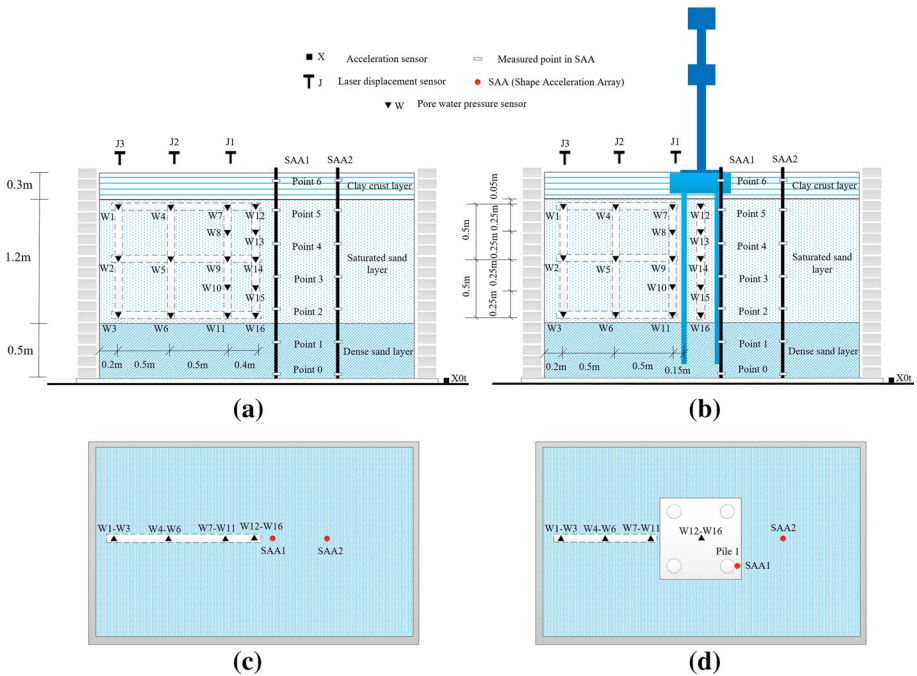
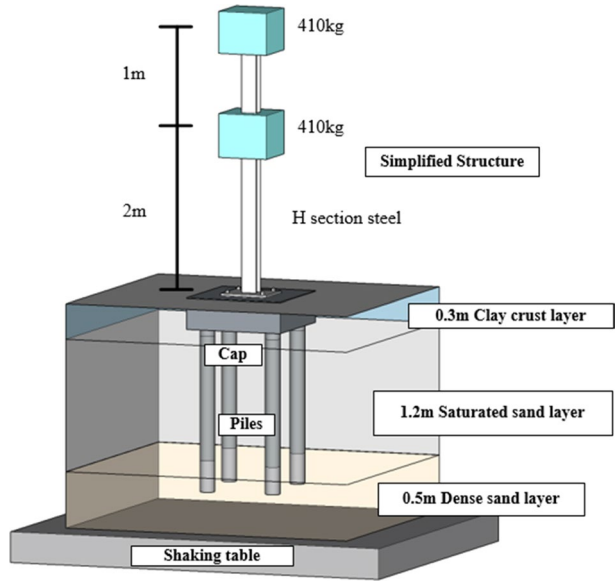


Fig. 3 Layout of test package and instrumentation: **a** elevation view of free field; **b** elevation view of non-free field; **c** plan view of free field; and **d** plan view of non-free field

In this series of shaking table experiments, a sine beat wave with the acceleration amplitude of 0.05 g and the Wulong seismic record in Wenchuan Earthquake with the amplitude of 0.3 g is selected as the ground motions. The Wulong ground motion was recorded at the Wulong seismic station in Sichuan Province, China, during the Ms8.0 Wenchuan Earthquake (2008). It was chosen to represent a major earthquake record in order to observe the strong nonlinear response and failure mechanism of the whole dynamic interaction systems. The peak acceleration of Wulong ground motion record was scaled to 0.3 g. In order to induce larger dynamic response of the soil–structure system and ensure the occurrence of liquefaction, the duration of the signal was reduced by half, so that the main frequency of Wulong ground motion record became close to the predominant frequency of the sites.

White noise is chosen to obtain the dynamic characteristic of the model system before and after tests. The sine beat wave curve and the time history and the corresponding Fourier spectrum of Wulong seismic record which used in this series experiments are displayed in Figs. 4 and 5.

3 Dynamic characteristic of model systems

It should be noted that the dynamic characteristics of soils in both experiments were paid attention to, so the frequencies and damping ratios are all calculated from the data measuring by SAA2. SAA2 is the array consisted of several acceleration sensors as illustrating in Fig. 3. The natural frequency and damping ratio of the model system were calculated by transfer function and half-power bandwidth method (Clough and Penzien 1993), using acceleration data from the accelerometers at the bottom (SAA2 Point 0) and at the top (SAA2 Point 6). Before and after inputting seismic records, white noise with the amplitude of 0.05 g was inputted to sweep the frequency of the model system, and the natural frequencies and damping ratios of model systems in both experiments were obtained as listed in Table 1.

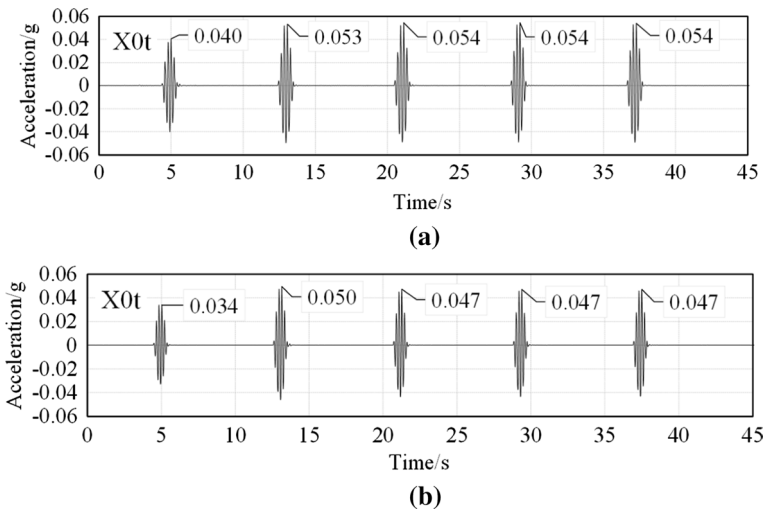


Fig. 4 Sine beat wave acceleration time history measuring by X0t: **a** in free field experiment; **b** in non-free field experiment

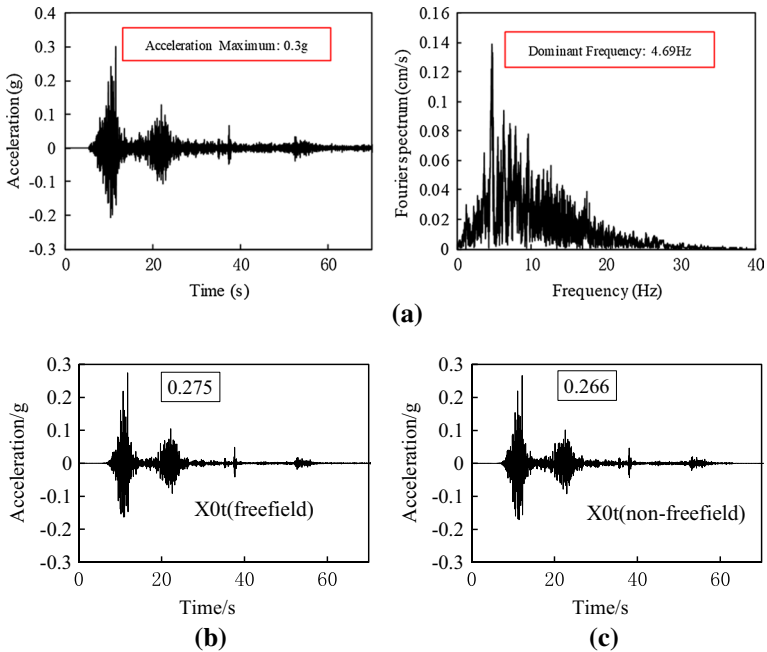


Fig. 5 Acceleration time history and corresponding Fourier spectra of Wolong ground motion record in Wenchuan Earthquake: **a** Target data; **b** X0t in free field experiment; **c** X0t in non-free field experiment

Table 1 Dynamic characteristics of model system in Experiment F and Experiment NF

Test events	Basic frequency (Hz)		Damping ratio (%)	
	Free field	Non-free field	Free field	Non-free field
White noise (before shaking test)	4.85	5.43	4.2	3.9
White noise (after shaking test)	4.52	4.84	5.4	4.2

As shown in Table 1, the natural frequencies of the model system obtained from the second white noise sweep (before the test) were smaller than that from the first white noise sweep (after the test), while the damping ratio is increased after the end of ground motions exciting.

The dynamic characteristics of non-free field and free field are different to some extent: due to the existence of structures made of materials with large stiffness, the natural frequency of free field is lower than that of non-free field, while the damping ratio of free field is higher than that of non-free field. The natural vibration frequency of the non-free field is large, but the damping is small, which indicates that the stiffness of the field will be increased and the energy dissipation capacity will be decreased to some extent in the presence of the structure.

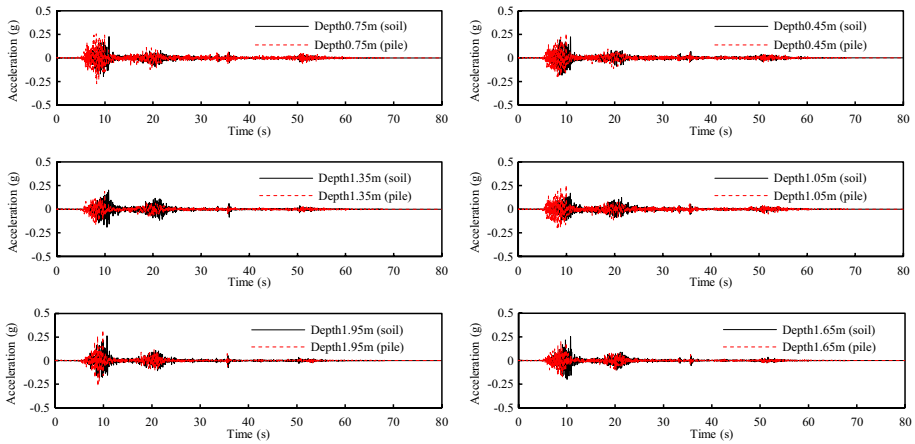


Fig. 6 Acceleration time histories of pile and soil in NF Experiment for 0.3 g Wolong ground motion record

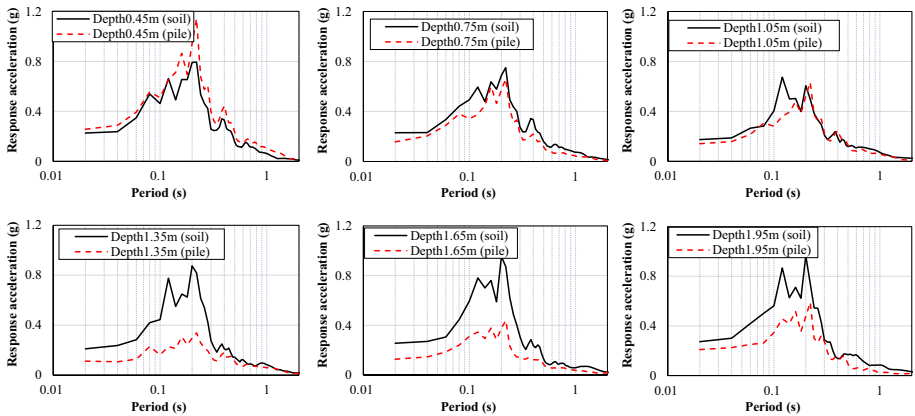


Fig. 7 Response spectra of pile and soil in NF Experiment for 0.3 g Wolong ground motion record

4 Soil–structure interaction in the non-free field

In the non-free field experiment, SAA1 and SAA2 were used to measure the acceleration response of the pile and soil, respectively. Actually, soil–structure dynamic interaction reflected in acceleration responses is that there are the differences in peak values of acceleration waveform and corresponding response spectrum. Figures 6 and 7 display the acceleration time histories and the corresponding spectra of 0.3 g Wolong ground motion record measuring by SAA1 and SAA2. It can be seen from the figures that the time-history waveforms and amplitudes of acceleration response of pile and soil at the same depth are different, and the response spectrum curves of corresponding measuring points are also obviously distinguishing. That is, the vibration of pile and soil is not consistent, and there is a phase difference between them, which indicates that the soil–structure dynamic interaction is very strong.

5 Porewater pressure responses

5.1 Porewater pressure development

The excess pore water pressure ratio was calculated by excess pore water pressure and the corresponding initial effective vertical stress as listed in the following formula (1). In fact, the data measured by pore pressure sensors are total pore water pressure, not excess pore water pressure. Excess pore water pressure is obtained by subtracting the hydrostatic pressure from the total pore water pressure. The initial effective vertical stress can be obtained by formula (2).

$$PPR = \frac{p_e}{p_{ini}} \tag{1}$$

where PPR is the excess pore water pressure ratio, p_e is the excess pore water pressure and p_{ini} is the corresponding initial effective vertical stress at the same position.

$$p_{ini} = (\rho_{sat} - \rho_w)hg \tag{2}$$

where ρ_{sat} is the saturated density of soils, ρ_w is the density of water, e is the void ratio of soils, h is the depth of measuring point, g is the acceleration due to gravity.

According to the porewater pressure data obtained from each measuring point, all of the porewater pressure ratios (PPRs) at different positions can be calculated, and then peak porewater pressure color nephograms were drawn in the software Surfer (Version 12.0). It's important to point out herein, that the porewater pressure sensors at W3 and W6 is damaged in Experiment-F and the porewater pressure sensor at W14 is damaged in Experiment-NF. Figures 8 and 9 display the peak porewater pressure color nephograms of saturated sand layer for 0.05 g sine beat wave and 0.3 g Wolong seismic record in both experiments.

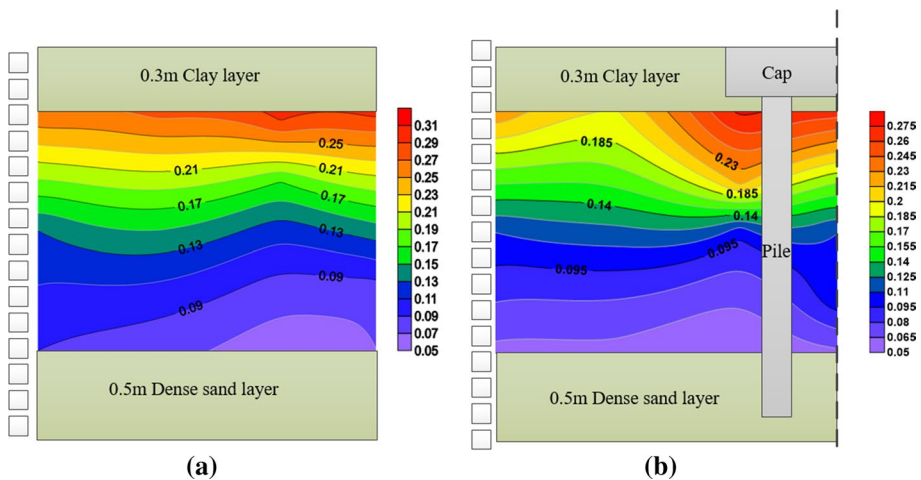


Fig. 8 Peak porewater pressure color nephograms for 0.05 g sine beat wave in: **a** Experiment-F; **b** Experiment-NF

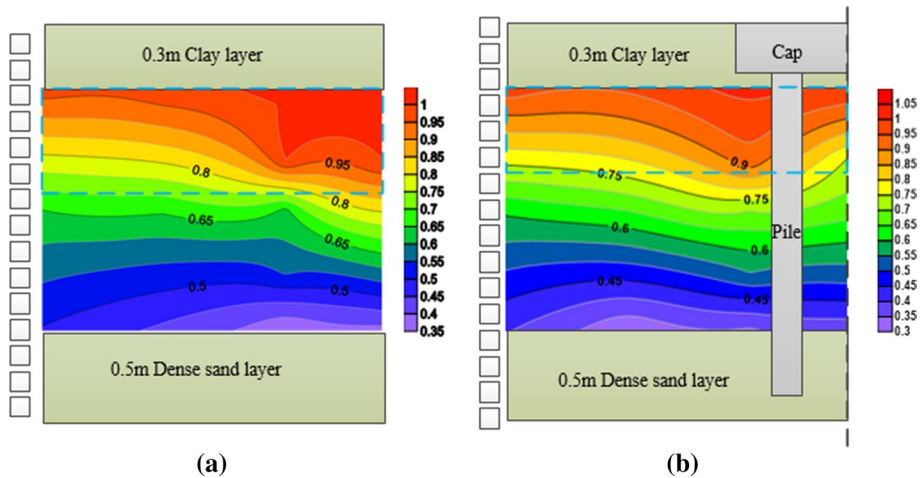


Fig. 9 Peak porewater pressure color nephograms for 0.3 g Wolong ground motion record in: **a** Experiment-F; **b** Experiment-NF

As shown in Fig. 8, porewater pressure ratios in saturated sand layer are all very small in both experiments for the test case of 0.05 g sine beat wave. The porewater pressure ratios in the upper of saturated sand layer are maximum and reach or close to 0.3. In fact, except the area near measuring point W7, the values of porewater pressure ratio at different positions are very close, and that is, the presence of the structure has little effect on the overall pore pressure reaction under the weak seismic loading.

Figure 9 illustrates the peak porewater pressure color nephograms 0.3 g Wolong seismic record, and the areas with pore pressure ratios greater than 0.8 has been circled by the dotted line. In both experiments, the peak porewater pressure ratios at measuring points W1 and W2 in the saturated sand layer are all smaller than that at other measuring points with the same height, which is caused by the gaps between soil and the container. By comparing Fig. 9a, b, it can be seen that the peak porewater pressure ratios at the same depth in the free field is slightly higher than that at the corresponding depth in the non-free field, and the liquefied soil area in the free field is significantly larger, that is, the liquefaction depth of the saturated sandy soil layer in the free field is deeper. The main reason for the differences is caused by the gaps due to the detachment and slippage between soil with piles and the cap during the strong vibration process, and the next section will continue the analysis at the viewpoint of pore pressure time history. In fact, the detachment and slippage should be caused by the vibration phase difference between pile–structure system and soil as the rule summarized from Fig. 9.

There are so many porewater pressure sensors embedded in the saturated sand layers, that the data measuring by the sensors located in the area with high porewater pressure ratios were analyzed herein, i.e. at the measuring points W4, W5, W7, W8, W12 and W13. The time histories of porewater pressure ratio at the six measuring points were illustrated in Figs. 10, 11 and 12.

From the porewater pressure responses at measuring points W4 and W5 far from the structure or the center of soil as shown in Fig. 10, the time-history waveforms and amplitudes of PPRs in this area are similar, and it shows that the pore pressure development of the non-free field is similar to that of the free field in fact. For the porewater pressure

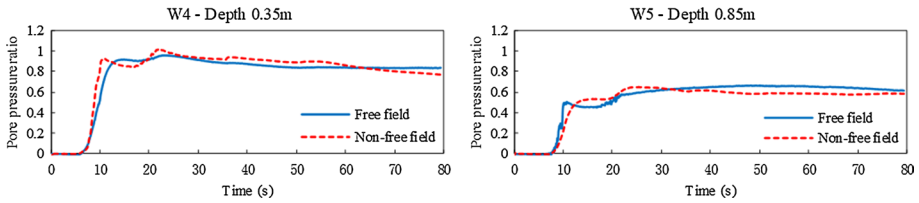


Fig. 10 Porewater pressure time histories at measuring points W4 and W5 (away from the structures or soil center)

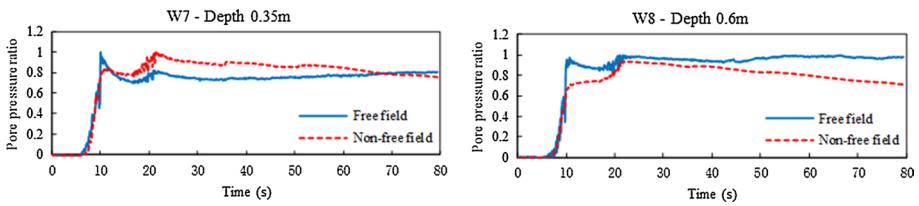


Fig. 11 Porewater pressure time histories at measuring points W7 and W8 (near the structures)

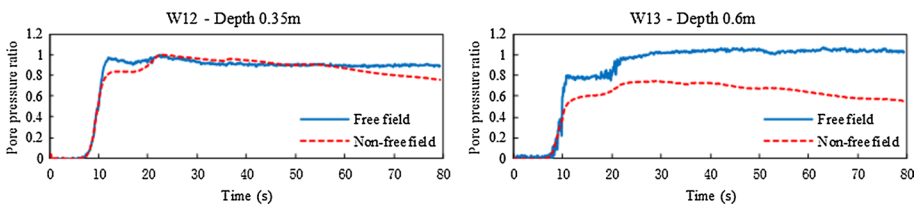


Fig. 12 Porewater pressure time histories at measuring points W12 and W13 (at the soil center or under the cap)

responses at the others measuring points as shown in Figs. 11 and 12, in the non-free field test, porewater pressure accumulation at the measuring points W7, W8, W12 and W13 close to the structure in the period from 5 to 13 s were at a low level and did not reach the peak porewater pressure ratio around the tenth second respectively. In the free field, the accumulation rates of porewater pressure are all faster than that of each pore pressure measuring point near the soil center. Compared with the pore pressure ratios at the same positions in the non-free field, the pore pressure ratio in the free field was generally higher at about 12 s. That is, during the period with strong shaking, the developments of pore pressure ratio are obviously affected due to the existence of structure, and it is difficult for the pore pressure ratio to reach a higher level in a short time.

For the time histories of pore pressure ratio after 35 s at each measuring point, it can be seen that the dissipation rates of pore pressure near the structure in the non-free field is obviously faster than that at the same positions in the free field, and the pore pressure ratios in the free field will stay at a very high level for a long time without obvious dissipation. Quantitative analysis of this is carried out in the following section.

It should be noted that the "waterspouts and sand boils" phenomenon was exhibited at the upper part of the measuring point W7 during the test, so the time-history curve of the

pore pressure ratio at the measuring point W7 suddenly decreased obviously to a smaller value when it was 10–20 s.

On the whole, in the Experiment-NF, the pore water pressure ratios near the structure is relatively small, and there is no rapid accumulation of porewater pressure due to soil–structure dynamic interaction. The main reasons should be that there are gaps in the interface between soil and structure since they are separated and slipped during the strong vibration process. In this series of shaking table tests, the structure system includes a pile-group foundation, so the pore water near the structure can dissipate upward through the contact surface between soil and the pile foundation and the pore water pressure is difficult to accumulate rapidly in the period of strong vibration. In fact, a large amount of water began to appear around the pile cap at about 15 s in the tests. Furthermore, there is no structure in the Experiment-F, and the upper layer is covered by a 0.3 m thick clay layer, so the porewater pressure cannot dissipate in a short time, even stays at a very high level for a long time after the end of the vibration loading.

5.2 Quantitative analysis on porewater pressure dissipation

Some studies (Davis and Berrill 1982b; Berrill and Davis 1985; He 1981; Guo and He 1992; Xu et al. 2019) discussed the effect of the shaking duration and seismic energy on liquefaction, and held the views that the duration of shaking should be an important and relevant parameter affecting soil liquefaction and porewater pressure would accumulate with increase of the energy of ground motions. In fact, for the duration of strong ground motion, many definitions of it based on seismic energy have been elucidated in some previous literatures. The definition of the duration of strong ground motion suggested by Trifunac and Brady (Hancock and Bommer 2007) is called significant duration, which defined by the time required for the energy of the ground motion to reach 5% to 95% of the total energy. This definition is mentioned and used herein for discussing the accumulation and dissipation of porewater pressure correlated with shaking energy of seismic loadings. For the seismic ground motion record measuring at the shaking table, i.e. at the measuring point X0t, the timing of reaching 5% total energy of the ground motion is at 7.55 s and that of reaching 95% is at 21.29 s as pointed at Fig. 13, and the significant duration is 13.74 s. As displaying in Figs. 10, 11 and 12, the peak porewater pressure ratios at different measuring points are all near the timings of acceleration peak amplitude or that of reaching 95% total energy of the ground motion. In particular, porewater pressure ratios keep at a high level in the period of the significant duration. The porewater pressure ratios at different timings are listed in Table 2. It should be noted that there are several specific timings were

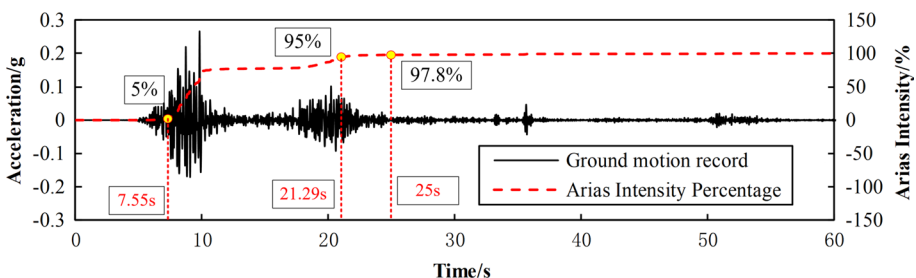


Fig. 13 Acceleration data measured at X0t and the corresponding Arias Intensity curve

Table 2 Porewater pressure at different timings and PPR dissipation rate at upper measuring points

Test scheme	Measuring point	Peak PPR	7.55 s (5%)	21.29 s (95%)	25 s (97.8%)	80 s (at the end)	PPR dissipation rate (%)
Free field	W4	0.96	0.09	0.93	0.95	0.83	12.06
	W5	0.66	0.00	0.55	0.59	0.61	- 3.62
	W7	1.00	0.13	0.80	0.77	0.81	- 5.30
	W8	1.00	0.04	0.95	0.98	0.98	0.35
	W12	1.00	0.04	0.98	0.96	0.89	7.14
	W13	1.00	0.01	0.85	0.91	0.96	- 5.82
Non-free field	W4	1.00	0.08	0.99	0.97	0.77	20.78
	W5	0.77	0.00	0.59	0.65	0.58	9.75
	W7	1.00	0.04	0.91	0.92	0.75	18.33
	W8	0.94	0.04	0.89	0.93	0.71	23.31
	W12	1.00	0.02	0.95	0.99	0.76	23.47
	W13	0.75	0.03	0.69	0.74	0.55	24.95

paid an attention to herein. The timing at the outset of strong shaking marks the beginning of steep accumulation of porewater pressure and PPRs at each measuring point increase obviously in the period from 7.55 to 21.29 s as shown in Table 2. In addition, the acceleration amplitudes and the shaking energy are all very small after 25 s, so the porewater pressure should show the trend of dissipation from this timing. The dissipation rates of porewater pressure in the period from 25 s to the end of recording porewater pressure time-histories were calculated in Table 2 and discussed as following.

As listed in Table 2, in the free field, the PPRs at the end of the seismic loading are all close to the corresponding peak PPR values at each measuring point. It shown that PPR dissipation rates at the measuring points in the free field are all small, except at W4. PPRs at several measuring points such as W8 and W12 increased slightly comparing with that at the time point 25 s, and this suggests that the pore pressure ratios in free field soil still keep at a high level for a certain time after the strong shaking period with high seismic energy and the development of porewater pressure even shows an accumulation trend.

For the PPR dissipation rates in non-free field listed in Table 2, the porewater pressures at each measuring point dissipated obviously from 25 to 60 s, and except that at W5, all of PPR dissipation rates reach around 20%. PPR dissipation at liquefied area in non-free field are significantly faster comparing with that in the free field.

The distance between measuring points W4, W5 and the pile is about 6.5 times the pile diameter as illustrated in Fig. 3. In fact, it also shown that the range of influence of structure on PPR in the liquefied site is very large from the discussion on the rules of PPR at W4 and W5. In this series of shaking table tests, it is no doubt that the PPR data measuring at W1, W2 and W3 were affected by the soil boundary, on account of porewater pressure dissipated from the surface between soil and the rubber membrane attached to the soil container. Therefore, rules of PPR at W4 and W5 reflect that the distance of the structural influence on the liquefied site was at least 6.5D away from the pile-group, from qualitative point of view.

6 Acceleration and response spectra

The acceleration amplification factor is the ratio of the peak acceleration at the measuring point to the peak acceleration of inputting seismic record at the bottom of the soil mass. The magnitude of the acceleration amplification factor indicates the amplification or damping effect of the soil on the seismic loadings. The acceleration data measured at each measuring point of SAA2 were used to calculate the acceleration amplification factor of soil mass in both experiments. Figure 14a, b shows the distribution diagram of the acceleration amplification factor of soil mass when 0.05 g sinusoidal beat wave and 0.3 g Wolong seismic record were input, respectively.

For the test case with 0.05 g sine beat wave, the acceleration responses of saturated sand layer and clay layer in both experiments showed a trend of continuous amplification from the bottom to soil surface and the acceleration amplification factor of the upper soil reached 2, which indicated the soil mass had an obvious amplification effect on the seismic loading. Moreover, the acceleration amplification factor of soil mass of the non-free field is slightly larger than that of the free field. But from the overall trends, the acceleration amplification factor of soil mass in both experiments differs little from each other. This shows that the existence of the structure has no obvious influence on the acceleration amplification effect of the soil under the weak seismic vibration.

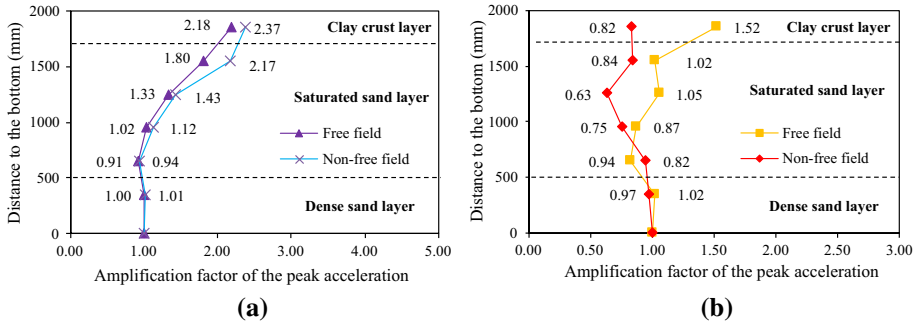


Fig. 14 Amplification factors of peak acceleration from SAA2 in both experiments for: **a** 0.05 g sine beat wave; **b** 0.3 g Wolong ground motion record

For the test case with the 0.3 g Wolong seismic record, the soil in both experiments all had no obvious amplification effect on the earthquake loading except for the topmost clay layer, but the magnitude and trend of acceleration amplification factor were significantly different. In the Experiment-F, the acceleration response at the lower part of the saturated sand layer has a certain decrease, while the upper part of the saturated sand layer has a small amplification effect on the earthquake loading. The acceleration amplification factor of the clay layer even reaches 1.52, which the acceleration response is significantly amplified here. For the Experiment-NF, acceleration amplification factor at each measuring point in soil mass is less than 1, and it shows that the acceleration response has no amplification at all positions in the soil. Moreover, the acceleration amplification factor in the middle and upper part of saturated sand layer and in the clay layer is obviously lower than that in the corresponding positions in the free field, which indicates that the existence of the structure significantly reduces the acceleration response of the field.

Figure 15 indicates the acceleration response spectra corresponding to each SAA2 measurement point in both experiments with the test case with 0.3 g Wolong earthquake record. It can be seen from Fig. 15 that the acceleration response spectra at SAA2-1 in the

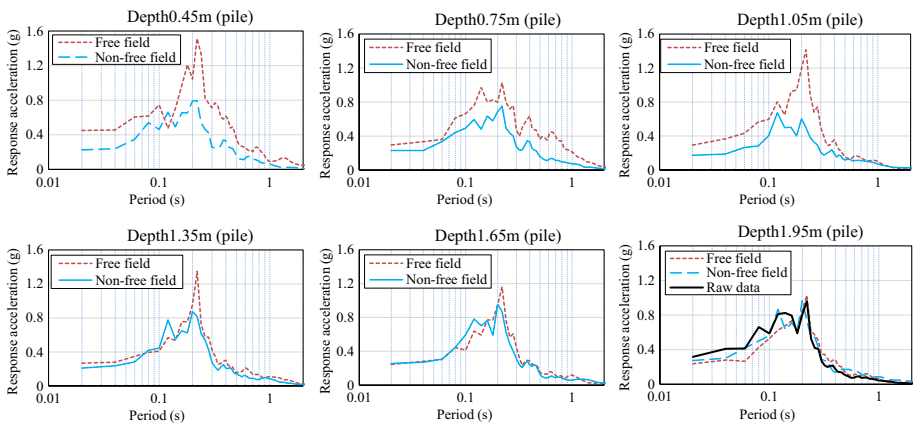


Fig. 15 Acceleration response spectra at SAA2 measuring points and raw data for 0.3 g Wolong ground motion record

dense sand layer in both experiments are very close to that of the input seismic record, and only part of the high-frequency components (which with period less than 0.1 s) are filtered, which is due to the high stiffness of the dense sand layer and SAA2-1 measurement point is near the bottom of the soil. In addition to the measuring point in the dense sand layer, the response spectra at the other measuring points in the free field are quite different from that of the input seismic record. Long-period components for a period greater than 0.15 s will be amplified to some extent, especially the reaction acceleration amplification near 0.2 s (corresponding to the frequency 5 Hz) are obvious. Compared with the response spectrum of the input seismic record, the acceleration response spectra of the measured points in the non-free field has almost the same, and the periodic components have no significant change.

Combining with the analysis on acceleration amplification factors, it can be summarized that the structure obviously changed the characteristic of the seismic loadings propagating in soil, and the amplitudes and periodic components of acceleration signals of the field change greatly due to the existence of the structure. Soil mass of the free field may have a certain amplification effect on seismic load and will enrich the long period ground motion components. In the non-free field, due to the soil–structure dynamic interaction, the peak values of acceleration decrease obviously in the field and its periodic components have no significant change. In the Experiment-NF, due to the far distance between SAA2 and the structure, and the liquefaction of the soil, the first two natural frequencies of the structure (corresponding to periods 0.7 s and 0.09 s) have no significant influence on the acceleration response spectra of soil.

7 Lateral displacement of soils

The lateral deformation of the soil can be measured and calculated by the inclinometers in SAA. Figure 16a, b, respectively, shows the distribution diagram of the lateral earth displacement amplitudes obtained by SAA2 for the test cases with 0.05 g beat wave and 0.3 g Wolong earthquake record in both experiments.

As shown in Fig. 16a, it can be found that the lateral deformation rule of soil in the free field is consistent with that in the non-free field, which is that the lateral displacements at

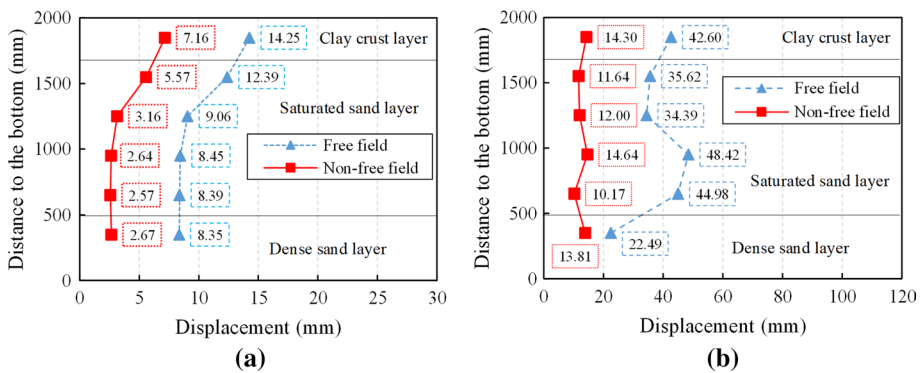


Fig. 16 Amplitude of lateral displacements of soils at SAA2 measuring points in both experiments for: **a** 0.05 g sine beat wave; **b** 0.3 g Wolong ground motion record

the upper soil are all large and lateral displacements at the lower part of soil mass are small and almost the same. In the free field, the lateral displacement amplitudes of all of the soil are much larger than that in the non-free field. The lateral displacements of the soil in the free field is 5–6 mm larger than that in the non-free field. The lateral displacement of the clay layer and the upper part of saturated sand layer in the free field is 12–14 mm, while the maximum lateral displacement at the same position in the non-free field is only 5–7 mm.

Figure 16b shows the distribution of lateral displacement amplitudes of soil for the test case with the 0.3 g Wolong earthquake record, and the soil displacements for the test case with the 0.3 g Wolong earthquake record was significantly greater than that for the test case with the 0.05 g beat wave as illustrated in Fig. 16a, b. The lateral displacements of the non-free field soil are about 10 mm to 15 mm, and the lateral displacement amplitudes of soils, except at the measured point in the dense sand layer, are all 40 mm approximately. Due to the existence of structure in the non-free field, the lateral displacement of the soil at each measuring point from top to bottom differs little. In the free field, the lateral displacement of the soil in the dense sand layer is the smallest and that at the lower part of the saturated sand layer is the largest, and it shows the rule with the amplitudes from the bottom up varied from small to large and then decreased. It should be because the stiffness of the dense sand layer is large, so the deformation is small. The lateral displacement of the lower part of the saturated sand layer is large due to the possible relative sliding at the interface of the soil layers as well as the small soil stiffness, and the vibration isolation effect of clay layer and the upper part of saturated sand due to soil liquefaction, it causes that the lateral displacements in the middle and upper soil layer is smaller than that in the lower soil. To sum up, the existence of the structure significantly reduces the lateral displacement response of the field soil.

Combined with the results of acceleration and porewater pressure response in both experiments above, it can be seen that the existence of pile group-superstructure system reduce the dynamic response of the surrounding liquefiable soil and significantly improves the aseismic stability.

8 Conclusions

By comparing the experimental results of the free field and non-free field experiments, the differences of soil acceleration, porewater pressure and lateral displacement between the test groups of free field and non-free field were discussed and analyzed, and the experimental results shown that the dynamic characteristics, seismic responses and aseismic stability of the soil are all distinguishing caused by the existence of structure. The existence of a structure actually will reduce the seismic responses of the liquefiable site and is beneficial to improve the aseismic stability of the field with liquefiable sandy soil layer. The conclusions summarized from experimental results provide an important reference for liquefaction analysis, and the main conclusions are as followings:

- (1) For the weak seismic loading condition, the rule of porewater pressure ratio is similar in both experiments. During strong shaking process, the porewater pressure near the structure accumulated more slowly and PPR is hard to reach a higher level in a short time in the non-free field. In the free field, the saturated sand is more prone to liquefaction and the depth of liquefaction is also larger. This rule indicates that soil–structure dynamic interaction cause the liquefiable sand layer harder to liquefy.

- (2) After strong shaking, the porewater pressures dissipate more rapidly in the non-free field, especially that near the structure. The existence of the structure will accelerate the dissipation rate of porewater pressure.
- (3) Compared with seismic responses of the free field, the acceleration response and lateral displacement of soil in the non-free field are significantly smaller. That is, the field is less likely to fail and the aseismic stability is improved.
- (4) The influence range of the structure on the seismic response of soil such as acceleration and the development of porewater pressure as well as lateral displacement of soil reaches 6.5 times the pile diameter at least.

Besides, it also suggests from discussion and analysis that substructure analysis method used in the study of soil–structure dynamic response may underestimate the aseismic stability of the field soil, due to the extracted free field response obviously greater than that of the ground around the actual structural system, and cause that the calculated result will differ greatly from the real responses. It is no doubt that this series of shaking table experiments is qualitative one and proceeding precise quantitative analysis based on the data from shaking table tests to reflect the rules of any prototype site is difficult, and quantitative and further analysis on more problems such as the influence range of the pile-group on the development of porewater pressure in liquefied soil calls for refined numerical model to research.

Author contributions PD: formal analysis, writing—original draft. CX: conceptualization, resources, methodology, investigation, writing—original draft. XD: supervision, data curation, validation, writing—review & editing. SC: supervision, writing—review & editing.

Funding This work was supported by the Foundation for Innovative Research Groups of the National Natural Science Foundation of China (Grant No. 51421005), the National Natural Science Foundation of China (Grant No. 51578026) and the National Science Fund for Excellent Young Scholars of China (Grant No. 51722801). The authors gratefully acknowledge the financial support from those projects.

Availability of data and material All of the data and material in the manuscript are available from the corresponding author.

Declarations

Conflict of interest All of authors declare that they have no known competing financial interests or personal relationships that could have appeared to influence the work reported in this paper. All authors named in the paper have participated in this work and agreed for the manuscript to be submitted to BEE.

References

- Berrill JB, Davis RO (1985) Energy dissipation and seismic liquefaction of sands: revised model. *Soils Found* 25(2):106–118. https://doi.org/10.3208/sandf1972.25.2_106
- Boulanger RW, Curras CJ, Kutter BL et al (1991) Seismic soil–pile–structure interaction experiments and analysis. *J Geotech Geoenviron Eng ASCE* 125(9):750–759. [https://doi.org/10.1061/\(ASCE\)1090-0241\(1999\)125:9\(750\)](https://doi.org/10.1061/(ASCE)1090-0241(1999)125:9(750))
- BS En 1998-5 (2004) Eurocode8: design of structures for earthquake resistance, part 5: foundation, retaining structure and geotechnical engineering. BSI, London, p 2004

- Cetin KO, Youd TL, Seed RB et al (2004) Liquefaction induced lateral spreading at Izmit Bay during the Kocaeli (Izmit)-Turkey Earthquake. *J Geotech Geoenviron Eng* 130(12):1300–1313. [https://doi.org/10.1061/\(ASCE\)1090-0241\(2004\)130:12\(1300\)](https://doi.org/10.1061/(ASCE)1090-0241(2004)130:12(1300))
- Chen G, Li F (2006) Probabilistic estimation of sand liquefaction based on neural network model of radial basis function. *Chin J Geotech Eng* 28(3):301–305. [https://doi.org/10.1016/S1872-1508\(06\)60035-1](https://doi.org/10.1016/S1872-1508(06)60035-1) (in Chinese)
- Chen G, Chen S, Qi C et al (2015) Shaking table tests on a three-arch type subway station structure in a liquefiable soil. *Bull Earthq Eng* 13(6):1675–1701. <https://doi.org/10.1007/s10518-014-9675-0>
- Cheng Z, Dafalias YF, Manzari MT (2013) Application of SANISAND Dafalias–Manzari model in FLAC3D. In: The 3rd international FLAC/DEM symposium at: Hangzhou, China. Volume: continuum and distinct element numerical modeling in geomechanics. Itasca International, Inc. https://www.researchgate.net/publication/283503214_Application_of_SANISAND_Dafalias-Manzari_model_in_FLAC3D
- Chiaradonna A, Flora A, D’Onofrio A, Bilotta E (2020) A pore water pressure model calibration based on in-situ test results. *Soils Found* 60(2):327–341. <https://doi.org/10.1016/j.sandf.2019.12.010>
- Clough RW, Penzien J (1993) Dynamics of structures, 2nd edn. McGraw-Hill, New York
- Dafalias YF, Manzari MT (2004) Simple plasticity sand model accounting for fabric change effects. *J Eng Mech* 130(6):622–634. [https://doi.org/10.1061/\(ASCE\)0733-9399\(2004\)130:6\(622\)](https://doi.org/10.1061/(ASCE)0733-9399(2004)130:6(622))
- Davis RO, Berrill JB (1982a) Energy dissipation and seismic liquefaction in sands. *Earthq Eng Struct Dyn* 10:59–68. <https://doi.org/10.1002/eqe.4290100105>
- Davis RO, Berrill JB (1982b) Energy dissipation and seismic liquefaction in sands. *Earthq Eng Struct Dyn* 10(1):59–68. <https://doi.org/10.1002/eqe.4290100105>
- Di Ludovico M, Chiaradonna A, Bilotta E, Flora A, Protta A (2020) Empirical damage and liquefaction fragility curves from 2012 Emilia earthquake data. *Earthq Spectra* 36(2):507–536. <https://doi.org/10.1177/8755293019891713>
- Dobry R, Ladd RS, Powell D et al (1982) Prediction of pore water pressure build up and liquefaction of sands during earthquakes by the cyclic strain method. NBS Building Science Series 138, National Bureau of Standards, Maryland. <https://nehrpsearch.nist.gov/static/files/NIST/PB83111617.pdf>
- Du XL, Lu DC (2011) Advances in soil dynamics and geotechnical earthquake engineering. *Rock Soil Mech* 32(S2):10–20. <http://ytlx.whrsm.ac.cn/CN/article/downloadArticleFile.do?attachType=PDF&id=10594> (in Chinese)
- El Naggar MH, Novak M (1994a) Non-linear model for dynamic axial pile response. *J Geotech Eng* 120(2):308–329. [https://doi.org/10.1061/\(ASCE\)0733-9410\(1994\)120:2\(308\)](https://doi.org/10.1061/(ASCE)0733-9410(1994)120:2(308))
- El Naggar MH, Novak M (1994b) Nonlinear lateral interaction in pile dynamics. *Soil Dyn Earthq Eng* 14:141–157. [https://doi.org/10.1061/\(ASCE\)0733-9410\(1994\)120:4\(678\)](https://doi.org/10.1061/(ASCE)0733-9410(1994)120:4(678))
- El Shamy U, Zeghal M, Dobry R et al (2010) Micromechanical aspects of liquefaction-induced lateral spreading. *Int J Geomech* 10(5):190–201. [https://doi.org/10.1061/\(ASCE\)GM.1943-5622.0000056](https://doi.org/10.1061/(ASCE)GM.1943-5622.0000056)
- Elsawy MK, El Naggar MH, Cerato AB et al (2019) Data reduction and dynamic p–y curves of helical piles from large-scale shake table tests. *J Geotech Geoenviron Eng ASCE* 145(10):04019075. [https://doi.org/10.1061/\(ASCE\)GT.1943-5606.0002146](https://doi.org/10.1061/(ASCE)GT.1943-5606.0002146)
- Fukutake K, Ohtsuki A, Sato M et al (1990) Analysis of saturated dense sand-structure system and comparison with results from shaking table test. *Earthq Eng Struct Dyn* 19(7):977–992. <https://doi.org/10.1002/eqe.4290190705>
- Gao X, Ling X, Tang L et al (2011) Soil–pile–bridge structure interaction in liquefying ground using shake table testing. *Soil Dyn Earthq Eng* 31(10):9–17. <https://doi.org/10.1016/j.soildyn.2011.03.007>
- Guo Y, He GN (1992) Relationship between dynamic pore pressure and excited energy of light loam and its application to predicting site liquefaction potential. *J Dalian Univ Technol* 32(6):732–736. <https://doi.org/10.1007/BF02032915> (in Chinese)
- Hadush S, Yashima A, Uzuoka R (2000) Importance of viscous fluid characteristics in liquefaction induced lateral spreading analysis. *Comput Geotech* 27(3):199–224. [https://doi.org/10.1016/S0266-352X\(00\)00015-X](https://doi.org/10.1016/S0266-352X(00)00015-X)
- Haeri S, Kavand A, Rahmani I et al (2012) Response of a group of piles to liquefaction-induced lateral spreading by large scale shake table testing. *Soil Dyn Earthq Eng* 38:25–45. <https://doi.org/10.1016/j.soildyn.2012.02.002>
- Halder S, Babu GLS (2010) Failure mechanisms of pile foundations in liquefiable soil: parametric study. *Int J Geomech* 10(2):74–84. [https://doi.org/10.1061/\(ASCE\)1532-3641\(2010\)10:2\(74\)](https://doi.org/10.1061/(ASCE)1532-3641(2010)10:2(74))
- Hancock J, Bommer JJ (2007) Using spectral matched records to explore the influence of strong-motion duration on inelastic structural response. *Soil Dyn Earthq Eng* 27(4):291–299. <https://doi.org/10.1016/j.soildyn.2006.09.004>

- Hayashi K, Kaneda S (2019) Nonlinear response and damage monitoring of a concrete pile as a result of soil liquefaction. *Struct Eng Int* 3:370–376. <https://doi.org/10.1080/10168664.2018.1562314>
- He GN (1981) Energy analysis procedure for evaluating soil liquefaction potential. *Chin J Geotech Eng* 3(4):11–21. http://manu31.magtech.com.cn/Jwk_ytgxcb/CN/Y1981/V3/I4/11
- Holzer TL, Bennett MJ, Ponti DJ et al (1999) Liquefaction and soil failure during 1994 Northridge earthquake. *J Geotech Geoenviron Eng* 125(6):438–452. [https://doi.org/10.1061/\(ASCE\)1090-0241\(1999\)125:6\(438\)](https://doi.org/10.1061/(ASCE)1090-0241(1999)125:6(438))
- Horikoshi K, Thakareet SW et al (2003) Performance of piled raft foundations subjected to dynamic loading. *Int J Phys Model Geotech* 3(2):51–62. <https://doi.org/10.1680/ijpmg.2003.030205>
- Huang Y, Atsushi Y, Feng Z (2005) Finite element analysis of pile soil structure dynamic interaction in liquefiable site. *Chin J Geotech Eng* 27(6):646–651. <https://doi.org/10.3321/j.issn:1000-4548.2005.06.008>
- Kramer S, Sideras S, Greenfield M (2016) The timing of liquefaction and its utility in liquefaction hazard evaluation. *Soil Dyn Earthq Eng* 91:133–146. <https://doi.org/10.1016/j.soildyn.2016.07.025>
- Li ZM (2011) Effect of previous cyclic axial loads on pile groups. *Int J Phys Model Geotech* 12(1):15–23. <https://doi.org/10.1680/ijpmg.2012.12.1.15>
- Li G, Motamed R (2017) Finite element modeling of soil–pile response subjected to liquefaction-induced lateral spreading in a large-scale shake table experiment. *Soil Dyn Earthq Eng* 92:573–584. <https://doi.org/10.1016/j.soildyn.2016.11.001>
- Lombardi D, Bhattacharya S (2014) Modal analysis of pile-supported structures during seismic liquefaction. *Earthq Eng Struct Dyn* 43(1):119–138. <https://doi.org/10.1002/eqe.2336>
- Lombardi D, Bhattacharya S (2016) Evaluation of seismic performance of pile-supported models in liquefiable soils. *Earthq Eng Struct Dyn* 45(6):1019–1038. <https://doi.org/10.1002/eqe.2716>
- Matsumoto T, Fukumura K, Horikoshi H, Oki A (2004) shaking table tests on model pile rafts in sand considering influence of superstructures. *Int J Phys Model Geotech* 4(3):21–38. <https://doi.org/10.1680/ijpmg.2004.040302>
- Mokhtar A, Abdel-Motaa M, Wahidy M (2014) Lateral displacement and pile instability due to soil liquefaction using numerical model. *Ain Shams Eng J* 5(4):1019–1032. <https://doi.org/10.1016/j.asej.2014.05.002>
- Morz Z, Norris VA, Zienkiewicz OC (1981) An anisotropic critical state model for soils subjected to cyclic loading. *Geotechnique* 31(4):451–470. <https://doi.org/10.1680/geot.1981.31.4.451>
- Motamed R, Towhata I (2010a) Shaking table model tests on pile groups behind quay walls subjected to lateral spreading. *J Geotech Geoenviron Eng ASCE* 136(3):477–489. [https://doi.org/10.1061/\(ASCE\)GT.1943-5606.0000115](https://doi.org/10.1061/(ASCE)GT.1943-5606.0000115)
- Motamed R, Towhata I (2010b) Mitigation measures for pile groups behind quay walls subjected to lateral flow of liquefied soil. *Soil Dyn Earthq Eng* 30(10):1043–1060. <https://doi.org/10.1016/j.soildyn.2010.04.016>
- Motamed R, Towhata I et al (2009) Behavior of pile group behind a sheet pile quay wall subjected to liquefaction-induced large ground deformation observed in shaking test in E-defense project. *Soils Found* 49(3):459–475. <https://doi.org/10.3208/sandf.49.459>
- Motamed R, Sesov V, Towhata I et al (2010) Experimental modeling of large pile groups in sloping ground subjected to liquefaction-induced lateral flow 1-g shaking table tests. *Soils Found* 50(2):261–279. <https://doi.org/10.3208/sandf.50.261>
- National Research Council (1985) Liquefaction of soils during earthquakes. National Academy Press, Washington DC
- Okamura M, Teraoka T (2006) Shaking table tests to investigate soil desaturation as a liquefaction countermeasure. *Seismic Perform Simul Pile Found* 132(2):282–293. [https://doi.org/10.1061/40822\(184\)23](https://doi.org/10.1061/40822(184)23)
- Pastor M, Zienkiewicz OC, Chen HC (1990) Generalized plasticity and the modeling of soil behavior. *Int J Numer Anal Methods Geotech*. <https://doi.org/10.1002/nag.1610140302>
- Qiu Z, Lu J, Elgamal A et al (2019) OpenSEES three-dimensional computational modeling of ground-structure systems and liquefaction scenarios. *Comput Model Eng Sci* 120(3):629–656. <https://doi.org/10.32604/cmescs.2019.05759>
- Ramirez J, Barrero AR, Chen L, Dashti S et al (2018) Site response in a layered liquefiable deposit: evaluation of different numerical tools and methodologies with centrifuge experimental results. *J Geotech Geoenviron Eng* 144(10):04018073. [https://doi.org/10.1061/\(ASCE\)GT.1943-5606.0001947](https://doi.org/10.1061/(ASCE)GT.1943-5606.0001947)
- Sasaki Y, Towhata I, Tokida K et al (1992) Mechanism of permanent displacement of ground caused by seismic liquefaction. *Soil Found* 32(3):79–96. https://doi.org/10.3208/sandf1972.32.3_79
- Seed HB, Idriss IM (1971) A simplified procedure for evaluating soil liquefaction potential. *J Soil Mech Found Div* 97(9):1249–1273. <https://doi.org/10.1061/JSFEAQ.0001662>

- Seed HB, Idriss IM, Arango I (1983) Evaluation of liquefaction potential using field performance data. *J Geotech Eng* 109(3):458–482. [https://doi.org/10.1016/S1872-1508\(06\)60035-1](https://doi.org/10.1016/S1872-1508(06)60035-1)
- Seed HB, Tokimatsu K, Harder LF et al (1985) Influence of SPT procedures in soil liquefaction resistance evaluations. *J Geotech Eng* 111(12):1425–1445. [https://doi.org/10.1061/\(ASCE\)0733-9410\(1985\)111:12\(1425\)](https://doi.org/10.1061/(ASCE)0733-9410(1985)111:12(1425))
- Sonmez B, Ulusay R (2008) Liquefaction potential at Izmit Bay: comparison of predicted and observed soil liquefaction during the Kocaeli earthquake. *Bull Eng Geol Env* 67:1–9. <https://doi.org/10.1007/s10064-007-0105-2>
- Stringer M, Madabhushi G (2011) The effect of pile installation method on dynamic pile response. *Int J Phys Modelling in Geotechnics* 11(3):87–99. <https://doi.org/10.1680/ijpmpg.2011.11.3.87>
- Stringer ME, Madabhushi SPG (2013) Axial load transfer in liquefiable soils for free-standing piles. *Géotechnique* 63(5):400–409. <https://doi.org/10.1680/geot.11.P.078>
- Su L, Tang L, Ling X et al (2015) Responses of reinforced concrete pile group in two-layered liquefied soil–shake–table investigations. *J Zhejiang Univ Sci A* 16(2):93–104. <https://doi.org/10.1631/jzus.a1400093>
- Suzuki H, Tokimatsu K, Sato M et al (2005) Factor affecting horizontal subgrade reaction of piles during soil liquefaction and lateral spreading. In: *Workshop of Seismic Performance and Simulation of Pile Foundations in Liquefied and Laterally Spreading Ground*: University of California, Davis, California, vol 3, pp 16–18. [https://doi.org/10.1061/40822\(184\)1](https://doi.org/10.1061/40822(184)1)
- Tabata K, Sato M (2010) E-defense shaking table test on the behavior of liquefaction-induced lateral spreading of large-scale model ground with a pile-foundation structure behind quay wall. In: *International conferences on recent advances in geotechnical earthquake engineering and soil dynamics*, vol 8, no 4, pp 1–6. <https://scholarsmine.mst.edu/icrageesd/05icrageesd/session08/4/>
- Tobita T, Iai S, Rollins KM et al (2004) Group pile behaviour under lateral loading in centrifuge model tests. *Int J Phys Model Geotech* 4(4):1–11. <https://doi.org/10.1680/ijpmpg.2004.040401>
- Tsai CC, Lin WC, Chiou JS (2016) Identification of dynamic soil properties through shaking table tests on a large saturated sand specimen in a laminar shear box. *Soil Dyn Earthq Eng* 83:59–68. <https://doi.org/10.1016/j.soildyn.2016.01.007>
- Varghese R, Latha G (2014) Shaking table studies on the conditions of sand liquefaction. *Geo-congress technical papers*, vol 234, pp 1244–1253. <https://doi.org/10.1061/9780784413272.121>
- Varun AD (2012) A generalized hysteresis model for biaxial response of pile foundations in sands. *Soil Dyn Earthq Eng* 32(1):56–70. <https://doi.org/10.1016/j.soildyn.2011.08.004>
- Xu CS, Dou PF, Gao LC et al (2019) Shaking table test on effects of ground motion duration compression ratio on seismic response of liquefied foundation. *Rock Soil Mech* 40(1):147–155. <https://doi.org/10.16285/j.rsm.2017.2342> (in Chinese)
- Xu CS, Dou PF, Du XL et al (2020a) Seismic performance of pile group-structure system in liquefiable and non-liquefiable soil from large-scale shake table tests. *Soil Dyn Earthq Eng* 138(11):106299
- Xu CS, Dou PF, Du XL et al (2020b) Large shaking table tests of pile-supported structures in different ground conditions. *Soil Dyn Earthq Eng* 139(12):106307
- Ye B, Yokawa H, Kondo T et al (2006) Investigation on stiffness recovery of liquefied sandy ground after liquefaction using shaking-table tests. In: *Proceedings of sessions of GeoShanghai: pavement mechanics and performance*, Reston, Virginia, U.S.A., ASCE Press. [https://doi.org/10.1061/40862\(194\)64](https://doi.org/10.1061/40862(194)64)
- Yiagos AN, Prevost JH (1991) Two-phase elasto-plastic seismic response of earth dams: theory. *Soil Dyn Earthq Eng* 10(7):357–370. [https://doi.org/10.1016/0267-7261\(91\)90025-U](https://doi.org/10.1016/0267-7261(91)90025-U)
- Youd TL, Garriss CT (1995) Liquefaction-induced ground surface disruption. *Journal of Geotechnical Engineering* 121(11):805–809. [https://doi.org/10.1061/\(ASCE\)0733-9410\(1995\)121:11\(805\)](https://doi.org/10.1061/(ASCE)0733-9410(1995)121:11(805))
- Youd TL, Idriss IM, Andrus RD et al (2001) Liquefaction resistance of soils: summary report from the 1996 NCEER and 1998 NCEER/NSF workshops on evaluation of liquefaction resistance of soils. *J Geotech Geoenviron Eng* 127(4):297–313. [https://doi.org/10.1061/\(ASCE\)1090-0241\(2001\)127:4\(297\)](https://doi.org/10.1061/(ASCE)1090-0241(2001)127:4(297))
- Zhuang H, Hu Z, Wang X et al (2015) Seismic responses of a large underground structure in liquefied soils by FEM numerical modelling. *Bull Earthq Eng* 13:3645–3668. <https://doi.org/10.1007/s10518-015-9790-6>